Mixed-symmetry states in ^{144}Nd: Semimicroscopic accounting within the cluster vibration model and its mapping into the interacting boson model

R. A. Meyer
Nuclear Chemistry Division, Lawrence Livermore National Laboratory, Livermore, California 94550 and Institut für Kernphysik II, Kernforschungsanlage Jülich GmbH, 5170 Jülich-1, Federal Republic of Germany

O. Scholten
Kernfysisch Versneller Institut, Rijksuniversiteit Groningen, 9747 AA Groningen, The Netherlands

S. Brant*
Institut für Kernphysik, Kernforschungsanlage D-5170 Jülich, Federal Republic of Germany

V. Paar
Prirodoslovno-Matematički Fakultet, University of Zagreb, 41000 Zagreb, Yugoslavia
(Received 11 May 1989)

We have investigated the structure of ^{144}Nd$_{84}$ within the framework of the cluster vibration model. Further, we have mapped, approximately, the cluster vibration model states into the proton-neutron interacting-boson model, with particular emphasis on the mixed-symmetry states, hindered transitions, quadrupole moment signs, and higher-angular-momentum pairs. The cluster vibration model 2^+ (3) state and its properties correspond to the experimentally determined properties and map into the mixed-symmetry state of the proton-neutron interacting-boson model. We compare the calculations with recent in-beam (t,p) multiparameter (particle, gamma, gamma/conversion-electron) coincidence studies, which have established the positive-parity spectra up to 3 MeV. Some evidence is given for 0^+ and 1^+ levels associated with the 2^+ (3) mixed-symmetry state.

I. INTRODUCTION

Because of the nearness of the $N=82$ closed shell, the excited state structure of ^{144}Nd$_{84}$ can be used to test both microscopic and geometric models.[1–5] Recent experimental investigations[2–7] of ^{144}Nd have sizably increased the body of data for this nucleus, which was studied in several earlier experimental investigations.[8–20] Inelastic scattering experiments[21] have led to the identification of a 1^+ mixed-symmetry state at 3075 keV in ^{156}Gd which possesses a large $B(M1)$ value of $1.3\pm0.2\mu_N$. This new degree of freedom, i.e., neutron versus proton oscillations or mixed-symmetry states, was recently carried to the $N=84$ nuclei, ^{140}Ba, ^{142}Ce, and ^{144}Nd, by Hamilton and co-workers,[1] who showed that the properties of the $2^+(3)$ state in these nuclei were consistent with their being mixed-symmetry states. The exploration of the full extent of the influence of this new degree of freedom on the low-energy spectra requires a detailed knowledge of the number and nature of ^{144}Nd levels up to ~3 MeV. Unfortunately, none of the experimental studies reported to date have been able to provide sufficiently detailed information on levels with energies greater than ~2 MeV. However, this situation has been resolved by recent multiparameter in-beam gamma-ray and conversion-electron spectroscopy studies.[22,23] Previous calculations for ^{144}Nd, however, performed by coupling two valence-shell neutrons to quadrupole bosons[20,24,25] and in the interacting boson model (IBA),[3,5] show poor correspondence with the level structure.

With two neutrons in the neutron valence shell and an open proton valence shell, ^{144}Nd provides a good test case for the study of models which are based on a boson picture. Complete bosonization implies a bosonization of both proton and neutron degrees of freedom. A fruitful approach based on this idea is provided by the IBA.[26,27] In the IBA-2,[27] a distinction is made between neutron and proton bosons, while in IBA-1,[26] one type of boson incorporates both proton and neutron excitations. As is well known, the IBA-2 model can reproduce the states of IBA-1 as symmetric in proton and neutron bosons, but in addition, it contains the states of mixed symmetry.

In the case of nuclei with two neutrons (or protons) outside a singly-closed-shell core nucleus, it is feasible to apply also an alternative, partial bosonization. In this case, the two neutrons (or protons) are treated as fermions, while the bosonization is performed only for the other valence shell. The cluster vibration model[28–30] (CVM) can describe the ^{144}Nd nucleus by coupling two valence-shell neutrons to the quadrupole boson core. In the CVM calculations, additional simplifying assumptions are also made: Quadrupole bosons are assumed to be harmonic, and the boson-fermion interaction is taken in its simplest form of dynamical particle-vibration coupling. Thus, the matrix elements of the Hamiltonian do not depend on the maximum number of quadrupole bosons, N, at which the quadrupole boson space is truncated. We note that in CVM the anharmonicities are not due to interaction between proton bosons, but are generated by the two-neutron cluster and proton boson, i.e., by the proton-neutron interaction. This is in agreement with the investigations in the IBA framework.[27,31]

Here, we report on our CVM calculations for ^{144}Nd and compare the results with our present experimental knowledge of the ^{144}Nd level structure. We then reinvestigate the problem of describing this nucleus in the framework of the IBA. In a further step, we discuss a mapping of CVM states into IBA-2. Particular attention is paid to the properties of the $2^+(3)$ state, which is not of the IBA-1 type and which has recently been successfully discussed in the framework of IBA-2 as a mixed-symmetry state.

II. CALCULATION OF ^{144}Nd WITHIN THE CVM

In the CVM, the nucleus ^{144}Nd is described by coupling two valence-shell neutrons to the quadrupole vibrational core. The following CVM Hamiltonian is employed:

$$H = H_{SM} + H_{\mathrm{QB}} + H_{\mathrm{res}} + H_{\mathrm{CBI}} \ . \tag{1}$$

Here, H_{SM} describes two independent valence-shell particles, which are referred to as the cluster; H_{QB} represents free quadrupole bosons; and H_{res} is the residual interaction between the particles in the cluster. We employ the pairing interaction as a residual interaction. The term H_{CBI} represents the cluster-quadrupole boson interaction, which has the form of a standard particle-vibration interaction, summed over particles of the cluster. Details of the model can be found in Refs. 28–30 and 32. Generally, by varying the number of particles in the cluster, one can describe the sequence of nuclei going away from a singly closed shell. However, because of the computational limitations, the model has been systematically used only for $n \le 3$.

Earlier calculations for ^{144}Nd in the framework of this approach have been reported in Refs. 20, 24, and 25. Here, we perform a more complete calculation, and compare the results with experimental levels up to 3 MeV.

The parameters appearing in the diagonalization of the CVM Hamiltonian are the following: single-particle energies, quadrupole boson energy, pairing strength, and the fermion-boson coupling strength. These parameters correspond to those that appear in the well-known Kisslinger-Sorensen model.[33] The parameters are as follows. The neutron single-particle energies in the $N = 82-126$ shell are taken from Ref. 34, as determined from the transfer reaction ^{142}Nd$(d,p)^{143}$Nd:

$$e(p_{1/2}) - e(f_{7/2}) = 2.13 \text{ MeV} ,$$

$$e(p_{3/2}) - e(f_{7/2}) = 1.34 \text{ MeV} ,$$

$$e(f_{5/2}) - e(f_{7/2}) = 1.85 \text{ MeV} ,$$

$$e(h_{9/2}) - e(f_{7/2}) = 1.34 \text{ MeV} ,$$

$$e(i_{13/2}) - e(f_{7/2}) = 1.6 \text{ MeV} .$$

The energy of the quadrupole boson is $\hbar\omega = 1.3$ MeV, which is about 15% lower than the energy of the 2_1^+ state in the singly-closed-shell $Z = 60$ core nucleus ^{142}Nd$_{82}$. Generally, such renormalization in CVM calculations reflects the renormalization of the boson field due to the presence of the cluster.[30,32] The pairing strength $G = 0.175$ MeV is chosen in accordance with the standard estimates. The particle-vibration coupling strength, a, is 0.7 MeV. This value is close to the value $a = 0.8$ used in the CVM calculation for nuclei with two neutrons in the $N = 50-82$ shell[35] and is in accordance with the estimate obtained by using $\langle k \rangle = 50$ and the measured $B(E2)(2_1^+ \to 0_1^+)$. Here $k(r) = r(dV/dr)$, where $V(r)$ is the single-particle potential energy.

The CVM Hamiltonian (1) is diagonalized in the basis

$$|(j_1 j_2)J, n_d R; I\rangle \ . \tag{2}$$

Here, j_1 and j_2 are two-neutron single particles that are coupled to the angular momentum J, and n_d is the number of quadrupole bosons that are coupled to the angular momentum R. The angular momenta J and R are coupled to the total angular momentum I. Included in the computation are the boson states up to $n_d = 3$ with unperturbed energies less than 7 MeV.

III. EXPERIMENTAL LEVELS AND COMPARISON WITH CVM RESULTS

As mentioned above, in-beam particle-gamma-(gamma/conversion-electron)-time multiparameter coincidence studies have recently been performed, using the (t,p) reaction.[22,23] Preliminary analysis of the results, when combined with the results of previous studies, has established the nature of ^{144}Nd levels up to ~ 3 MeV in excitation energy. The presently known levels in this energy range are shown in Fig. 1.

The calculated spectrum is also shown in Fig. 1 and compared with the experimental levels up to 2.9 MeV. We have computed the electromagnetic properties using the calculated wave functions and the standard CVM form of the $E2$ and $M1$ operator.[32] The effective charges and gyromagnetic ratios were chosen in accordance with Ref. 32 and are as follows: The neutron single-particle effective charge, $e_{\mathrm{s.p}}^{(n)} = 0.5$; boson effective charge, $e_{\mathrm{vib}} = 2.7$; boson gyromagnetic ratio $g_R = Z/A = 0.42$, and the orbital and spin gyromagnetic ratios for neutrons are, respectively, $g_l = 0$, and $g_s = 0.5 g_s^{\mathrm{free}} = -1.91$. Table I presents a comparison of the calculated electromagnetic properties with the experimental data. As seen in Fig. 1 and Table I, the calculated CVM results for energy levels and electromagnetic properties agree well with the available experimental data.

Initial analysis[23] of the data from the recent in-beam multiparameter has revealed some important features of the excited-state spectra of ^{144}Nd. The lowest-energy 1^+ level occurs at 2655 keV in the experimental spectrum. Previously, its identification was obfuscated by the fact that it forms a level doublet, with the 1^+ occurring at 2654.9 keV and a 3^+ occuring at 2654.6 keV. These two levels were identified earlier in separate investigations. The 2654.9-keV level was identified in[7] $(n,n'\text{-}\gamma)$ and beta-decay[2] studies with deexcitating transitions of 1958 and 2655 keV. The in-beam work can set the multipolarity of a third, previously unidentified transition to the $2^+(3)$ level as being $M1/E2$, while the beta-decay study sets $J=1$ and the $(n,n'$-$\gamma)$ investigation confirms the assignment as 1^+. The neutron-capture gamma-ray investigations of Snelling and Hamilton[5] establish a level at 2654.6 keV and set a 3^+ value based on their angular correlation data. Again, the in-beam data can confirm this level as well as the observations of Snelling and Hamilton of transitions to levels different from those observed for the deexcitation of the 2654.9-keV 1^+ level.

More important, the in-beam studies can establish, from gamma-gamma coincidence data, that the 2655-keV 1^+ level populates the $2^+(3)$ mixed-symmetry state. The transition probability for the population of the $2^+(3)$ mixed-symmetry state is ~ 30 times that of the other transitions depopulating the 2654.9-keV level. Also, as shown in Fig. 2, the in-beam studies populate the 0^+ level at 2743 keV. This level was observed to have an $l=0$ angular distribution in the (t,p) studies of Chapman *et al.*[12] and has been identified as being populated in the $^{144}\mathrm{Pm}^g$ (0^-) beta decay.[2] Unfortunately, the latter study's sensitivity was limited to identifying only the 1182- and 2048-keV transitions. As shown in Fig. 2, the in-beam gamma-ray and conversion-electron studies have not only identified an $E2$ transition to the $2^+(3)$ mixed-symmetry state but also show an $E0$ transition to the $0^+(2)$ level at 2084 keV. When the relative transition probabilities are compared, this level populates the $2^+(3)$ mixed-symmetry state ~ 20 times more readily than the $2^+(1)$ state. Thus, these observed properties suggest that this 0^+ state may be a member of the mixed-symmetry set of states. Elsewhere, we discuss these and other features, such as the preferential population of mixed-symmetry states in the (t,p) in-beam studies.[22,23]

IV. IBA-1 CALCULATION FOR ^{144}Nd

Two IBA-1 calculations for ^{144}Nd, which were performed using two different parametrizations,[3,5] have been reported so far. The basic difference between them lies in the treatment of the $2^+(3)$ state. Krane *et al.*[3] did not include the $2^+(3)$ state in the fitting. In the theoretical spectrum thus obtained, the theoretical counterpart of the $2^+(3)$ experimental level was missing. Snelling and Hamilton[5] chose the parametrization in such a way that a theoretical $2^+(3)$ state was obtained in the energy range

TABLE I. Comparison of calculated and experimental electromagnetic properties of ^{144}Nd.

Quantity	Experiment	Theory
$B(E2)[2^+(1)\to 0^+(1)]$ $(e^2\mathrm{b}^2)$	0.102 ± 0.003	0.106
$B(E2)[4^+(1)\to 2^+(1)]$ $(e^2\mathrm{b}^2)$	0.08 ± 0.01	0.122
$Q[2^+(1)]$ $(e\,\mathrm{b})$	-0.39 ± 0.21	-0.40
$\mu[2^+(1)]$ (μ_N)	0.33 ± 0.08	0.45
$\frac{I[2^+(2)\to 0^+(1)]}{I[2^+(2)\to 2^+(1)]}$	0.095 ± 0.001	0.10
$\delta[2^+(2)\to 2^+(1)]$	-1.13 ± 0.22	-1.70
$\frac{B(E2)[2^+(2)\to 0^+(1)]}{B(E2)[2^+(2)\to 2^+(1)]}$	$0.007^{+0.003}_{-0.001}$	0.007
$\frac{I[2^+(3)\to 0^+(1)]}{I[2^+(3)\to 2^+(1)]}$	0.43 ± 0.01	0.41
$\delta[2^+(3)\to 2^+(1)]$	0.31 ± 0.11	0.38
$\frac{B(E2)[2^+(3)\to 0^+(1)]}{B(E2)[2^+(3)\to 2^+(1)]}$	0.63 ± 0.45	0.39
$\frac{I[2^+(4)\to 0^+(1)]}{I[2^+(4)\to 2^+(1)]}$	0.24 ± 0.01	0.73
$\frac{I[3^+(1)\to 2^+(1)]}{I[3^+(1)\to 4^+(1)]}$	0.57 ± 0.01	0.32
$\delta[3^+(1)\to 2^+(1)]$	0.4 ± 02	0.25
$\delta[3^+(1)\to 4^+(1)]$	$-0.84^{+0.17}_{-0.92}$	-0.49
$B(E2)[2^+(2)\to 0^+(1)]$	0.001 ± 0.001	0.001
$B(E2)[2^+(2)\to 2^+(1)]$	0.095 ± 0.021	0.073
$B(E2)[2^+(2)\to 4^+(1)]$		0.001
$B(E2)[2^+(3)\to 0^+(1)]$	0.013 ± 0.003	0.007
$B(E2)[2^+(3)\to 2^+(1)]$	0.02 ± 0.01	0.018
$B(E2)[2^+(3)\to 4^+(1)]$		0.026
$B(E2)[2^+(3)\to 2^+(2)]$		0.001
$B(M1)[2^+(2)\to 2^+(1)]$	0.034 ± 0.012	0.013
$B(M1)[2^+(3)\to 2^+(1)]$	$0.28^{+0.54}_{-0.20}$	0.161
$B(M1)[2^+(3)\to 2^+(2)]$		0.220

of the experimental $2^+(3)$ state. However, there were two difficulties: (1) The theoretical decay pattern of this level was in disagreement with the measured one for the experimental $2^+(3)$ state, and (2) the calculation predicts a low-lying $0^+(2)$ state, without an experimental counterpart. Furthermore, in both calculations[3,5] the density of positive-parity states between 2 and 3 MeV is much lower than that experimentally observed. The levels $2^+(1)$, $2^+(2)$, $4^+(1)$, $6^+(1)$, and $8^+(1)$, however, were described rather well. Consequently, Snelling and Hamilton argued that the applicability of IBA-1 to ^{144}Nd proved inconclusive.

In this work, we have reinvestigated the IBA-1 treatment of ^{144}Nd, with particular attention to (1) the triplet of experimental states $2^+(3)$, $0^+(2)$, and $4^+(2)$, which lie at the energies 2.073, 2.084, and 2.110 MeV, respectively, and (2) the density of states in the range of 2 to 3 MeV of excitation energy. We found that only the $4^+(2)$ state and one of the remaining two states of the triplet can be reproduced in the IBA-1 calculation. In Fig. 1 we compare the CVM theoretical spectrum [Fig. 1(a)] and the experimentally known levels [Fig. 1(b)] with two fits that include the states $4^+(2)$, $0^+(2)$ [Fig. 1(c)] and $4^+(2)$, $2^+(3)$ [Fig. 1(d)]. As shown in Figs. 1(c) and 1(d), the counterpart of the third member of the triplet, $2^+(3)$ and $0^+(2)$, respectively, is missing. The calculated spectrum in Fig. 1(c) is qualitatively similar to the calculation by Krane *et al.*[3] The calculated $2^+(3)$ state appears about 1 MeV above the doublet $0^+(2)$, $4^+(2)$. The experimental $2^+(3)$ state does not have a theoretical counterpart, nor do several experimental states between 2 and 3 MeV. The calculated spectrum in Fig. 1(d) qualitatively resembles the calculation by Snelling and Hamilton.[5]

It should be stressed that any attempt to fit the $2^+(3)$ state leads to the lowering of the $0^+(2)$ state to the energy at which no experimental 0^+ state appears. On the other hand, the calculated gamma-deexcitation pattern of the $2^+(3)$ state reveals that this state does not correspond to the experimental $2^+(3)$ state. Thus, the parametrization employed in the calculation in Fig. 1(c) appears more appropriate than that used in the calculation in Fig. 1(d). As is well known, IBA-1 contains only the states that are symmetric in proton and neutron collective degrees of freedom, i.e., the states that are symmetric in proton and neutron bosons in IBA-2. The fact that the $2^+(3)$ state cannot be reproduced in IBA-1 indicates that this state is not symmetric in protons and neutrons, i.e., that it may correspond to the mixed-symmetry state of IBA-2 or may be a two-quasiparticle ($2qp$) state.

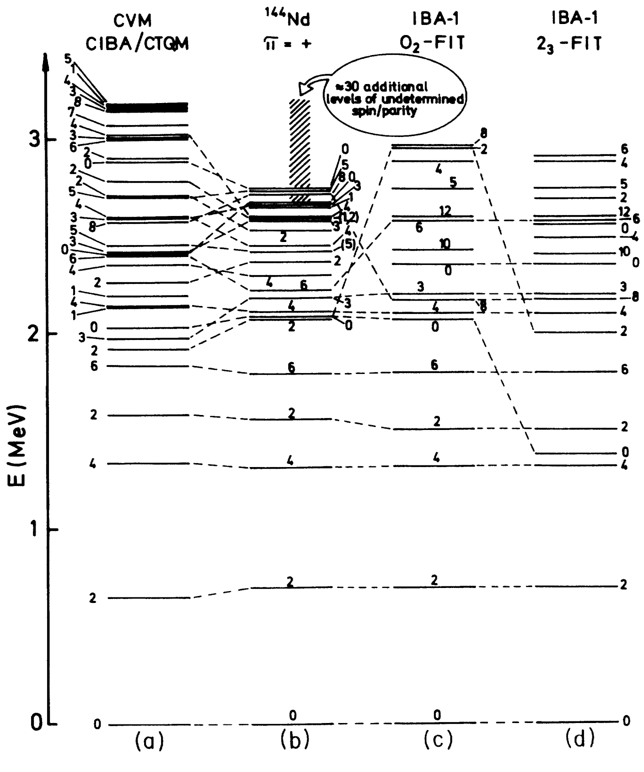

FIG. 1. Positive-parity levels theoretically predicted by the IBA and the CVM compared with the experimentally observed levels. (a) Theoretical spectrum in the CVM. (b) Experimentally known levels of ^{144}Nd. (c) Theoretical spectrum calculated in the IBA-1 by fitting to the experimental levels 2_1, 4_1, 2_2, 6_1, and 0_2. (d) Theoretical spectrum calculated in the IBA-1 by fitting to the experimental levels 2_1, 4_1, 2_2, 6_1, and 2_3.

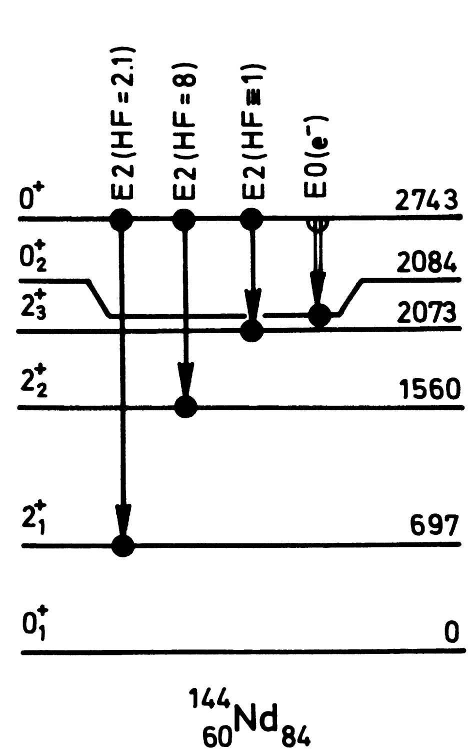

FIG. 2. Deexcitation of the 2743-keV level (N.B.: A dot at the arrowhead indicated that the transition has been established by its observation in the corresponding coincidence spectra). Hindrance factor is denoted by "HF."

V. MAPPING OF CVM INTO IBA-2

In mapping the results of the CVM calculation into the IBA-2 model, we are mainly concerned with the results for the neutrons. In the CVM the protons are already considered as a system of phonons that map directly into the proton bosons of the IBA-2 model by following the standard procedure of replacing the square root factors by s bosons, as for example

$$b^\dagger[(N-n_b)/N]^{1/2}|\,\rangle_{\text{CVM}} \to d^\dagger s|\,\rangle_{\text{IBA}} .$$

In the CVM model calculation for ^{144}Nd, the neutrons have been considered as two fermions in the 50–82 shell model basis. In mapping this two-neutron degree of freedom into the IBA model, we will follow the conventional approach of interpreting the neutron boson as the equivalent of a collective two-particle state. The microscopic structure of this collective pair can, for example, be determined from the neutron component of the $0^+(1)$ state calculated in the CVM. The two-particle, $J=0$ component in the wave function proportional to s^5 can be regarded as the equivalent of the neutron s boson, S_ν, while the neutron two-particle $J=2$ component multiplying the s^4d proton component should be regarded as the equivalent of the neutron d boson, D_ν. Table II lists the two-particle components of the neutron s and d boson thus determined. It can be seen that they are highly collective. Using this correspondence between the two-particle degree of freedom and the bosons, the wave function of the $0^+(1)$ state calculated in CVM can be written as

$$|0^+(1)\rangle_{\text{CVM}} = 0.75|s_\nu s_\pi^5\rangle + 0.51|(d_\nu d_\pi)^{(0)} s_\pi^4\rangle + \cdots .$$

These first two components reproduce 83% of the wave function. Of the remaining components, the dominant configurations are proportional to $|(d_\pi^2)^{(0)} s_\pi^3\rangle$ and $|(d_\pi^2)^{(2)} s_\pi^3\rangle$ and can be expressed to a very good approximation as $|s_\nu (d_\pi^2)^{(0)} s_\pi^3\rangle$ and $|d_\nu (d_\pi^2)^{(2)} s_\pi^3\rangle$ with amplitudes of 0.25 and 0.28, respectively. The coherence in the neutron part of the wave function multiplying the proton d_π^2 configuration has a collectivity very similar to those collectivities entering in the definition of the neutron s and d boson (given in Table II), i.e., the admixtures of so-called s' and d' components in the ground state are small. Together, these four IBA-like components reproduce 97% of the ground state function; over 97% of the CVM ground state wave function thus lies within the IBA model space.

The wave function of the $2^+(1)$ state can be analyzed in a similar way. The structure of a neutron s_ν boson can be determined from the two-particle wave function that is multiplied by the $|d_\pi s_\pi^4\rangle$ proton component, and similarly, the d_ν-boson structure can be determined from the $|s_\pi^5\rangle$ proton component. This procedure leads to a boson structure that is essentially indistinguishable from that given in Table II. Thus, in this way we have hereby verified the IBA assumption that the low-lying collective states are all built on similar collective two-particle states (the s and d bosons). In boson language, the wave function of the $2^+(1)$ state, as calculated in CVM, can be written as

$$\begin{aligned}|2^+(1)\rangle_{\text{CVM}} = {} & 0.624|s_\nu d_\pi s_\pi^4\rangle + 0.383|d_\nu s_\pi^5\rangle \\ & -0.14|s_\nu d_\pi^2 s_\pi^3\rangle - 0.245|d_\nu d_\pi s_\pi^4\rangle \\ & +0.2|d_\nu (d_\pi^2)^{(0)} s_\pi^3\rangle + 0.2|d_\nu (d_\pi^2)^{(2)} s_\pi^3\rangle \\ & +0.28|d_\nu (d_\pi^2)^{(4)} s_\pi^3\rangle + \cdots . \end{aligned} \quad (3)$$

The components quoted above reproduce 83% of the wave function. The higher components of this state contain $2qp$ neutron components. The $2qp$ $J=2$ neutron components are especially important. The probability of finding $2qp$ $J=4$ components (g bosons, in IBA language) is very small.

TABLE II. The structure of the neutron bosons as determined from CVM ground state wave functions.

Component	Amplitude
s_ν	
$(f_{7/2}^2)^{(0)}$	+0.778
$(p_{1/2}^2)^{(0)}$	+0.139
$(p_{3/2}^2)^{(0)}$	+0.339
$(f_{5/2}^2)^{(0)}$	+0.247
$(h_{9/2}^2)^{(0)}$	+0.323
$(i_{13/2}^2)^{(0)}$	−0.309
d_ν	
$(f_{7/2}^2)^{(2)}$	+0.628
$(f_{7/2},p_{3/2})^{(2)}$	−0.608
$(f_{7/2},f_{5/2})^{(2)}$	+0.136
$(f_{7/2},h_{9/2})^{(2)}$	−0.134
$(p_{1/2},p_{3/2})^{(2)}$	−0.187
$(p_{1/2},f_{5/2})^{(2)}$	−0.136
$(p_{3/2}^2)^{(2)}$	+0.214
$(p_{3/2},f_{5/2})^{(2)}$	−0.126
$(f_{5/2}^2)^{(2)}$	+0.104
$(f_{5/2},h_{9/2})^{(2)}$	−0.206
$(h_{9/2}^2)^{(2)}$	+0.140
$(i_{13/2}^2)^{(2)}$	−0.110

VI. LOW-ENERGY 2^+ STATES IN THE IBA AND CVM

Recently, the search for 2^+ states that are of mixed symmetry in the neutron-proton degree of freedom has received much attention. Hamilton *et al.*[1] have successfully described the $2^+(3)$ state of ^{144}Nd as a mixed-symmetry state of IBA-2. They showed that the gamma decay properties are consistent with those of the lowest mixed-symmetry state in the U(5) limit. In particular a strong experimental $2^+(3)$ to $2^+(1)$ $M1$ transition is consistent with a transition from a mixed-symmetry state to a fully symmetric state. In the CVM calculation, the experimental excitation energies and branching ratios are reproduced. It is thus interesting to investigate whether the $2^+(3)$ state in the CVM calculation indeed corresponds to a mixed-symmetry IBA-2 state. In particular, the competition between the collective and 2*qp* excitations in this energy regime can be studied.

In mapping the CVM wave functions into those of the IBA-2 model, the structure for the neutron boson should, in principle, be taken from Table II. The higher 2^+ levels contain considerable amplitudes outside the *s*-*d* IBA model space. Here, however, we are only interested in a qualitative analysis and will therefore not distinguish between the collective *s* and *d* bosons and the less collective s' and d' collective bosons, which have more 2*qp* components. This approach yields the following results for the lowest four 2^+ levels (for shortness of notation the *s* bosons are not written):

$$|2^+(1)\rangle_{\rm CVM}\approx 0.642|d_\pi\rangle+0.383|d_\nu\rangle +0.14|d_\pi^2\rangle+0.245|d_\nu d_\pi\rangle\ , \qquad (4)$$

$$|2^+(2)\rangle_{\rm CVM}\approx 0.13|d_\pi\rangle+0.46|d_\nu\rangle +0.37|d_\pi^2\rangle+0.49|d_\nu d_\pi\rangle\ , \qquad (5)$$

$$|2^+(3)\rangle_{\rm CVM}\approx -0.52|d_\pi\rangle+0.40|d_\nu\rangle -0.23|d_\pi^2\rangle-0.24|d_\nu d_\pi\rangle\ , \qquad (6)$$

$$|2^+(4)\rangle_{\rm CVM}\approx -0.25|d_\pi\rangle+0.44|d_\nu\rangle -0.29|d_\pi^2\rangle+0.18|d_\nu d_\pi\rangle\ , \qquad (7)$$

where components of higher order in n_d have been omitted. Since, for example, what is labeled as the $|d_\nu\rangle$ component of the $|2^+(2)\rangle_{\rm CVM}$ and the $|2_3^+\rangle_{\rm CVM}$ states consist only of about 50% of the same d_ν boson as given above, it is dangerous to draw quantitative conclusions. From the structure of the CVM wave functions, it can be seen that both the 2_3^+ and the 2_4^+ levels contain admixtures of $F=F_0-1$ components. These components are larger in the 2_4^+ state, where both the two $n_d=1$ and the two $n_d=2$ components differ in sign, as is typical for mixed-symmetry states. The CVM calculation thus suggests that the 2_4^+ state contains large mixed-symmetry components, although the admixture of 2*qp* components is large (perhaps of the order of 50%). These noncollective components may severely distort the simple IBA picture above 2 MeV of excitation energy.

The $0^+(1)$ and $2^+(1)$ states are almost free of 2*qp* admixtures and can therefore be used to test *F*-spin symmetry breaking. A direct measure of this is obtained by taking overlaps with states that do have good *F* spin:

$$|n_d=1,F=F_0\rangle=(\sqrt{N_\pi}|d_\pi\rangle+\sqrt{N_\nu}|d_\nu\rangle)/\sqrt{N}\ , \qquad (8)$$

$$|n_d=1,F=F_0-1\rangle=(\sqrt{N_\nu}|d_\pi\rangle-\sqrt{N_\pi}|d_\nu\rangle)/\sqrt{N}\ , \qquad (9)$$

$$|n_d=2,F=F_0\rangle=(\sqrt{N_\pi(N_\pi-1)}|d_\nu^2\rangle+\sqrt{2N_\nu N_\pi}|d_\nu d_\pi\rangle+\sqrt{N_\nu(N_\nu-1)}|d_\nu^2\rangle)/\sqrt{N(N-1)}\ , \qquad (10)$$

$$|n_d=2,F=F_0-1\rangle=(\sqrt{2N_\pi(N_\nu-1)}|d_\nu^2\rangle+(N_\pi-N_\nu)|d_\nu d_\pi\rangle-\sqrt{2N_\nu(N_\pi-1)}|d_\pi^2\rangle)/\sqrt{N(N-2)}\ , \qquad (11)$$

where $F_0=(N_\pi+N_\nu)/2$ is the maximum possible *F* spin. The overlaps of the CVM wave functions with these pure *F*-spin components can now be calculated, giving

$$\frac{\langle 0^+(1)|n_d=2;F=F_0\rangle}{\langle 0^+(1)|n_d=2;F=F_0-1\rangle}=1.9\ , \qquad (12)$$

$$\frac{\langle 2^+(1)|n_d=1;F=F_0\rangle}{\langle 2^+(1)|n_d=1;F=F_0-1\rangle}=9.0\ , \qquad (13)$$

$$\frac{\langle 2^+(1)|n_d=2;F=F_0\rangle}{\langle 2^+(1)|n_d=2;F=F_0-1\rangle}=2.2\ . \qquad (14)$$

The $n_d=0$ sector of the 0^+ level is, of course, fully symmetric. This decomposition of the wave function in the different *F*-spin components shows that the admixture of nonmaximal *F*-spin components is sizable.

VII. THE 1^+ AND 3^+ STATES

The study of 1^+ and 3^+ states is of great interest in relation to the question of mixed-symmetry states in the IBA model. In the IBA model, all 1^+ states necessarily have $F=F_0-1$, and finding these unambiguously fixes the position of mixed-symmetry states. In the CVM calculation, there are two kinds of 1^+ states possible: (1) those based on a 2*qp* excitation, and (2) collective 1^+ states involving similar collective two-particle structures as enter in the ground and first excited states. Only the latter can be related to the IBA model. For the 3^+ states, one should also clearly distinguish collective from 2*qp* excitations. These collective 3^+ states, however, are not so directly related to mixed-symmetry structures, since it is possible to have a $|n_d=3,F=F_0,J^\pi=3^+\rangle$ state beside the lowest mixed-symmetry $|n_d=2,F=F_0-1,J^\pi=3^+\rangle$ state.

Analysis of the CVM 1^+ wave functions shows that the states at $E_x=2.13$ and 2.20 MeV are dominated by 2*qp* components, while the $1^+(3)$ state at $E_x=3.17$ MeV is the collective state. The 2*qp* components of this collective state are negligible.

For 3^+ states, a clear separation also exists between collective and noncollective states. The first three 3^+ states are predominantly built on 2*qp* configurations, while the $3^+(4)$ state at 3.01 MeV is collective. It contains a mixture of a symmetric three *d*-boson component and a mixed-symmetry two *d*-boson component.

VIII. THE 4^+ AND 6^+ STATES

In most of the states that we have considered to far, the admixtures of collective $L=4$ (g boson) and $L=6$ (i boson) pairs are small. This is not the case, however, for the $4^+(1)$ and $6^+(1)$ levels: There can be large admixtures of these g and i bosons. The largest components of these states can be written as

$$|4^+(1)\rangle_{\rm CVM}=0.36|(d_\pi^2)^{(4)}\rangle +0.44|(d_\nu d_\pi)^{(4)}\rangle+0.45|g_\nu\rangle\ , \qquad (15)$$

$$|6^+(1)\rangle_{\rm CVM}=0.084|(d_\pi^3)^{(6)}\rangle+0.23|(d_\nu d_\pi^2)^{(6)}\rangle+ +0.45|(g_\nu d_\pi)^{(6)}\rangle+0.56|i_\nu\rangle\ , \qquad (16)$$

clearly showing the importance of high-angular-momentum pairs. It should be noted that the two-particle structure of the s_ν and d_ν components in these states is very similar to that of the $0^+(1)$ and $2^+(1)$ states. Table III gives the microscopic structure of the g_ν and i_ν pairs, and it can be seen that these exhibit a degree of collectivity similar to that of the d boson. This admixture of g_ν and i_ν bosons has two directly observable effects on the spectrum: (i) Energies of the $4^+(1)$ level and especially of the $6^+(1)$ level are much lower than expected in a purely vibrational spectrum, and in fact the spacing is more like what one would expect for a semiclosed shell model nucleus with $E(6^+)-E(4^+)<E(4^+)-E(2^+)<E(2^+)-E(0^+)$; and (ii) the $B(E2)$ values do not increase as one goes up the ground state band as would be expected in a vibrational nucleus, but instead, one has $B[E2;4^+(1)\to2^+(1)]\simeq B[E2;2^+(1)\to0^+(1)]$. In comparing these two effects with the data, one might even conclude that in the CVM calculation the admixture of the g_ν and i_ν pairs are underestimated. One should keep in mind, however, that the equivalent of a g_π boson has not been included in the present calculation.

TABLE III. Microscopic two-particle structures of the neutron g and i bosons as determined from the CVM wave function of the $4^+(1)$ and $6^+(1)$ states.

Component	Amplitude
g_ν	
$(f_{7/2}^2)^{(4)}$	+0.746
$(f_{7/2},p_{1/2})^{(4)}$	−0.207
$(f_{7/2},p_{3/2})^{(4)}$	−0.576
$(f_{7/2},f_{5/2})^{(4)}$	+0.093
$(f_{7/2},h_{9/2})^{(4)}$	−0.086
$(p_{1/2},h_{9/2})^{(4)}$	+0.062
$(p_{3/2},f_{5/2})^{(4)}$	−0.201
$(p_{3/2},h_{9/2})^{(4)}$	+0.082
$(f_{5/2}^2)^{(4)}$	+0.029
$(f_{5/2},h_{9/2})^{(4)}$	−0.037
$(h_{9/2}^2)^{(4)}$	+0.018
$(i_{13/2}^2)^{(4)}$	−0.004
i_ν	
$(f_{7/2}^2)^{(6)}$	+0.907
$(f_{7/2},f_{5/2})^{(6)}$	+0.354
$(f_{7/2},h_{9/2})^{(6)}$	−0.107
$(p_{3/2},h_{9/2})^{(6)}$	+0.197
$(f_{5/2},h_{9/2})^{(6)}$	−0.043
$(h_{9/2}^2)^{(6)}$	−0.012
$(i_{13/2}^2)^{(6)}$	+0.000

IX. HINDRANCE OF $2^+(2)$ TO $0^+(1)$ TRANSITION

We have investigated the hindrance of the $2^+(2)$ to $0^+(1)$ transition within the framework of the mapping of the CVM into the IBA. The reduction of the $2^+(2)$ to $0^+(1)$ transition moment in CVM is a consequence of the incoherence between fermion and boson contributions. In the leading order, these contributions are presented by the first-order cluster-type fermion diagram [Fig. 3(a)] and by the corresponding second-order induced boson-type diagram [Figs. 3(b)–(d)]. All these diagrams have the same topological structure, i.e., the corresponding contributions differ only in the energy denominators and the multiplication factor; the relative phases of these contributions are determined by the signs of the corresponding energy denominators. Thus, the induced collective diagrams [Figs. 3(b)–(d)] can be incorporated into the normalization of the fermion effective charge. The energy denominator for the parent diagram [Fig. 3(a)] is $1/\hbar\omega$ and for the induced collective diagram [Figs. 3(b)–(d)] it is

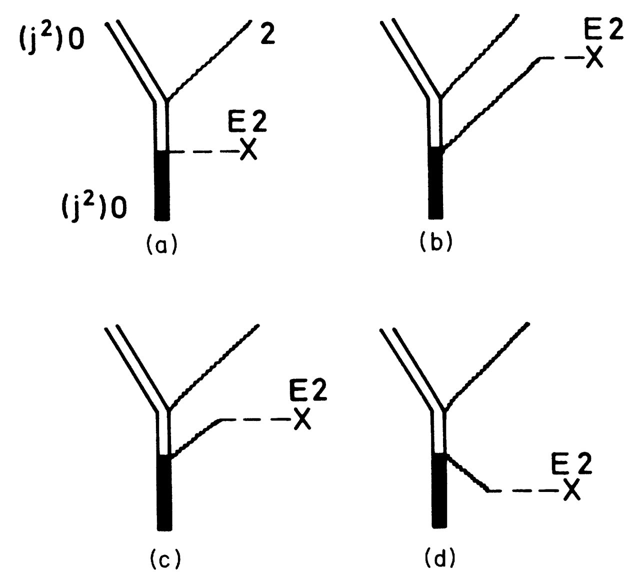

FIG. 3. Leading fermion- and boson-type diagrams contributing to the $2^+(2)\to0^+(1)$ transition in CVM. Full, wavy, and dashed lines denote the fermion, quadrupole boson, and $E2$ interaction, respectively.

$$[(-\Delta-\hbar\omega)(-\Delta-2\hbar\omega)]^{-1}+[(-\Delta-\hbar\omega)\hbar\omega]^{-1}+(-\tfrac{1}{2})(\hbar\omega)^{-2}=-(4\hbar\omega+\Delta)\cdot[2(\hbar\omega)^2(2\hbar\omega+\Delta)]^{-1} . \quad (17)$$

Here, $\hbar\omega$ denotes the energy of the quadrupole boson, and Δ is the pairing energy. As seen here, there is an incoherence among the boson contributions. Moreover, the sign of total induced boson-type contribution is opposite to the sign of the parent fermion-type contribution. This type of incoherence appears in the high-order perturbation terms too. As a consequence of this systematic incoherence, there arises a strong hindrance of the $2^+(2)$ to $0^+(1)$ transition. This hindrance is clearly reflected in the CVM computation for ^{144}Nd. The calculated ratio of the $2^+(2)$ to $0^+(1)$ and $2^+(2)$ to $2^+(1)$, $B(E2)$ values is

$$[B(E2;2_2^+\to 0_1^+)]/[B(E2;2_2^+\to 2_1^+)]=0.007 , \quad (18)$$

in agreement with the measured value. By performing the CVM to IBA-2 mapping, the CVM transition

$$|(j^2)2,12;2_2\rangle \to |(j^2)0,00;0_1\rangle \quad (19)$$

is mapped into the IBA-2 transition

$$|n_{d(\nu)}=1,n_{d(\pi)}=1,n_{s(\pi)}=N-2;2_2\rangle \to |n_{s(\nu)}=1,n_{s(\pi)}=N-1;0_1\rangle . \quad (20)$$

In this way, the hindrance of the $2^+(2)$ to $0^+(1)$ transition in nuclei near the U(5) limit appears in IBA-2 as a consequence of incoherence between the contributions to the $E2$ matrix element because of proton and neutron bosons.

X. THE SIGN RULE FOR STATIC QUADRUPOLE MOMENTS

The quadrupole moment of the $2^+(1)$ state arises in CVM because of the available two-particle cluster of angular momentum 2 and the positive response given by the boson "cloud," i.e., its main effect is a sizable enhancement of the cluster contribution.[32,36] A similar type of mechanism, in its simplest form, appears also for the quadrupole moment of the ground-state odd-mass nuclei with one particle (or hole) coupled to the quadrupole boson core.[37] The quadrupole moment of the ground state is then generated by the lowest-energy single particle (or hole), and is enhanced a few times by the quadrupole boson response. For example, such a mechanism gives rise to the quadrupole moment of ^{143}Nd$_{83}$: The quadrupole moment is generated by $Q_{\mathrm{s.p.}}(f_{7/2})\simeq -0.15$ e b, and is enhanced by the boson response to $Q(7/2_1^-)=-0.4$ e b.

The mechanism is somewhat more complex for even-even nuclei, which are described in CVM by coupling a two-particle cluster (two protons or two neutrons) to quadrupole bosons. In the case of ^{144}Nd, we have two valence-shell neutrons that are treated as a cluster, and ten protons in an open proton shell that are treated as quadrupole bosons. In this case, several two-particle cluster states of angular momentum 2 and positive parity are available, and they compete in generating the quadrupole moment of the $2^+(1)$ state. However, it turns out that the main contributions are given by two clusters only: the lowest two-particle state $|(j^2)2\rangle$ (where j is the lowest single-particle state in the valence shell of the cluster) and its non-spin-flip counterpart.[36,38,39]

For ^{144}Nd, the lowest-lying two-particle neutron state of angular momentum $J=2$ is $(f_{7/2}^2)2$. Its non-spin-flip counterpart is $(f_{7/2}p_{3/2})2$, because the matrix element

$$\langle (f_{7/2}p_{3/2})2||Y_2||(f_{7/2}^2)2\rangle$$

is of the non-spin-flip type. The matrix elements of Y_2 between $(f_{7/2}^2)2$ and all the other two-particle states available in the $N=82-126$ shell are of the spin-flip type, and therefore they are small or vanish.

The contributions to the quadrupole moment due to the two most important two-particle states are $Q[(f_{7/2}^2)2]>0$ and $Q[(f_{7/2}p_{3/2})]<0$. For a realistic choice of parameters [$e(p_{3/2})-e(f_{7/2})\simeq 1$ MeV, $\hbar\omega\simeq 1$ MeV, $a\simeq 1$ MeV] the second term dominates. Thus, the sign of the quadrupole moment of the $2^+(1)$ state is negative, opposite to that of the two neutron particles in the lowest single-particle configuration. Hence, any calculation which does not include the $p_{3/2}$ single-particle state, or places it too high, is bound to give a wrong sign of the quadrupole moment of the $2^+(1)$ state. Therefore, in order to reproduce the sign of the quadrupole moment of the $2^+(1)$ state, we have to include, in addition to $(f_{7/2}^2)2$, the $(f_{7/2}p_{3/2})2$ two-neutron state in mapping CVM to IBA-2. A neutron boson obtained by such mapping has a negative quadrupole moment, i.e.,

$$\langle d_\nu||M_B^{(\nu)}||d_\nu\rangle<0 . \quad (21)$$

The check of the consistency of this semimicroscopic deviation of the boson effective charge is given by the signs of quadrupole moments of the other states of the ground-state band. The sign of the boson charge, obtained from mapping the $2^+(1)$ state, predicts the negative IBA-2 quadrupole moments for all the other states of the ground-state band. This is in agreement with the results of CVM computation: $Q(4_1^+)=-0.57$ e b, $Q(6_1^+)=-0.80$ e b, $Q(8_1^+)=-1.01$ e b, and $Q(10_1^+)=-0.88$ e b.

XI. COMPARISON WITH IBA-2

In order to obtain a better insight into the structure of the low-energy states, we analyzed them in terms of the IBA-2 model. In fact, we have adjusted the parameters of the standard IBA-2 Hamiltonian,

$$H_{\mathrm{IBA-2}}=e_d n_d+\kappa Q_\nu Q_\pi \quad (22)$$

with

$$Q_\tau=(s^\dagger d+d^\dagger s)^{(2)}+\chi_\tau(d^\dagger d)^{(2)};\tau=\nu,\pi \ , \qquad (23)$$

in such a way as to reproduce the structure and energy of the ground state and the $2^+(1)$ state. The parameters thus deduced are $e_d=1.0$ MeV, $\kappa=-0.37$ MeV, and $\chi_\nu=-1.3$. The value of $\chi_\pi=0.0$ is taken to be the same as that used in the CVM calculation. It should be noted that the values of χ are not well determined by this procedure and could be changed by as much as 0.5. Such a change, however, will not greatly affect the structure and energies of the states that we will consider in the following discussion. It should also be noted that this procedure of constructing equivalent states in the IBA-2 model is only possible because the structures of both the ground state and the $2^+(1)$ state are dominated by configurations in which the neutrons are coupled to $J_\nu=0$ and $J_\nu=2$. The ground state only contains an admixture of 5.5% of configurations outside this S_ν,D_ν space (of which 5.1% is due to the $J=4$ component of g_ν pairs). For the $2^+(1)$ state, this non-S_ν,D_ν component is larger by about 14%, of which 12% is due to g_ν pairs. It is also important to note that the $J_\nu=2$ component in the $2^+(1)$ state has a shell model structure very similar to that of the $J_\nu=2$ component of the ground state. If this were not the case, the similarity to the IBA-2 model would have been lost.

The calculated energy spectrum in the IBA-2 model is given in Fig. 4, where it is compared with the spectrum as calculated in the CVM. In the latter model the level density is considerably higher than in the IBA model, as expected. In the IBA model, only those states are calculated that are built from a particular collective $J=0$ and $J=2$ two-particle state which corresponds to the s and d bosons. For example, the two 0^+ states calculated at 2.02 and 2.41 MeV are a mixture of the 0^+ state calculated in IBA at 2.27 MeV and a $2qp$ state with a similar unperturbed energy. The most important component of the $2qp$ state consists of a $J=0$ two-particle state which is orthogonal to the ground state. In some IBA calculations[40] this component is taken into account by including an s' boson. Similarly, the $2^+(2)$ state at 1.58 MeV in the CVM contains an important s' component. In the CVM, the 4^+ level is calculated at a considerably lower energy than in the IBA model because in the CVM this 4^+ level contains a rather important 40% contribution from

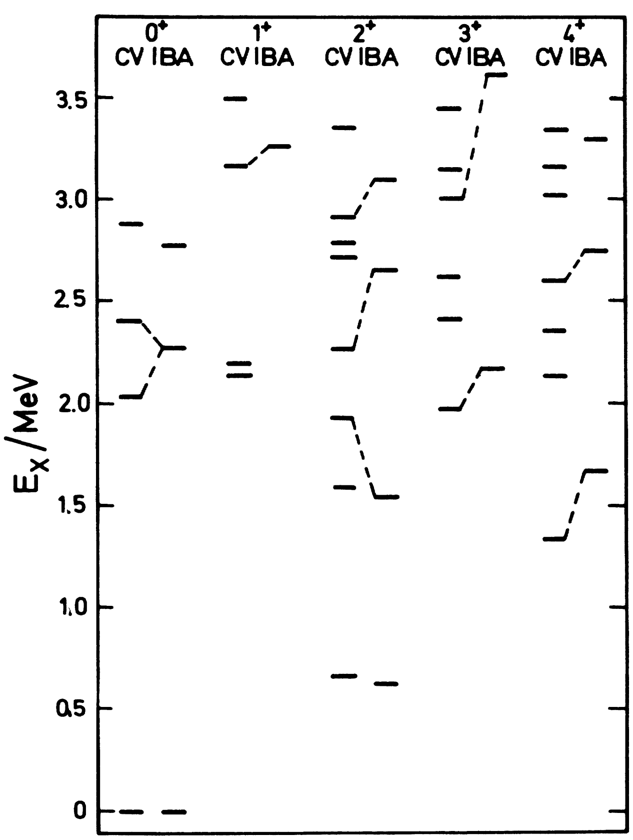

FIG. 4. Low-spin positive-parity levels theoretically predicted by the IBA-2 and the CVM.

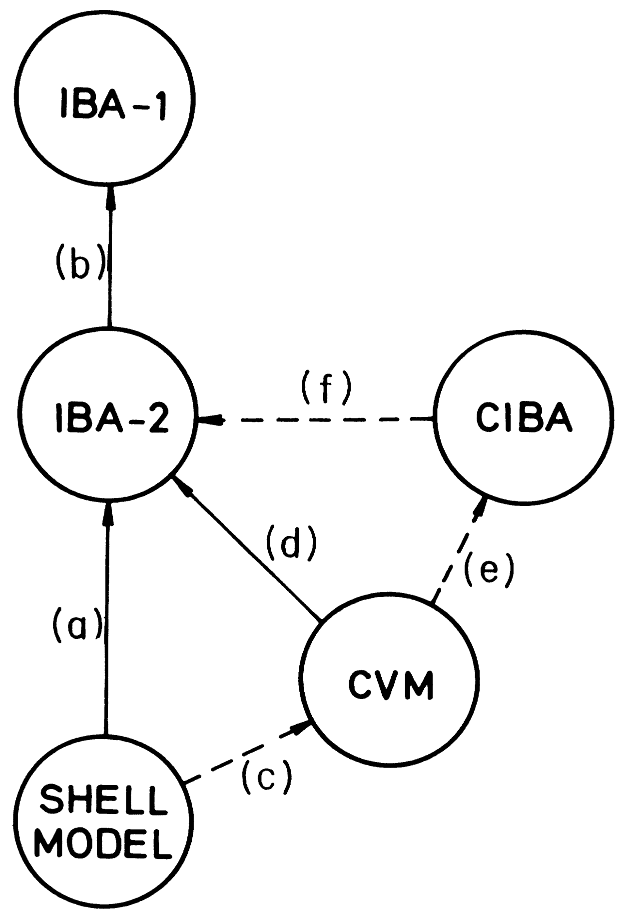

FIG. 5. The scheme of models referred to in the present discussion. Steps (a) and (b) have been the topics of numerous investigations in the framework of IBA (Ref. 27). In the present paper, step (d) is investigated.

$J_\nu=4^+$ pairs (the g_ν boson in the IBA model).

It is also interesting to investigate the neutron-proton symmetry structure of the states.[41] In both the CVM and IBA calculations, the $2^+(1)$ state has maximum F-spin symmetry.[42] In the CVM calculation, the $2^+(3)$ and $2^+(4)$ states both contain a relatively large admixture of mixed-symmetry components, as is the case with the corresponding $2^+(2)$ and $2^+(3)$ states in the IBA model. In the CVM calculation, therefore, it is not the $2^+(2)$ state, which can be considered primarily a $2qp$ excitation, but rather the higher-energy $2^+(3)$ and $2^+(4)$ states that correspond to the mixed-symmetry 2^+ states as predicted in the IBA model.[43] In addition, in the CVM spectrum the equivalent of the mixed-symmetry IBA-1^+ states can be found at 3.16 MeV with only a very small admixture of $2qp$, non-IBA-type states. The 1^+ states below 2.5 MeV in CVM are dominated by 1^+ $2qp$ configurations. In relation to the position of mixed-symmetry states in the spectrum, it is interesting to note that in the IBA Hamiltonian no Majorana force was used.

XII. CONCLUSION

We have investigated the structure of the ^{144}Nd$_{84}$ nucleus, and its mixed-symmetry states in particular, within the framework of both the CVM and the IBA. We have presented a mapping from the CVM into IBA-2 for the low-energy states. In particular, we have shown that the $2^+(4)$ state of CVM maps into the mixed-symmetry state of IBA-2.

We have also deduced a relation between the two models CVM and IBA and completed step (d) in the intermodel relationship diagram shown in Fig. 5. These two models have different scopes in the sense that the CVM is made to describe nuclei in the vicinity of a semiclosed shell. It explicitly treats noncollective neutron $2qp$ degrees of freedom in the case of ^{144}Nd. The IBA, on the other hand, is made to describe collective low-energy states. While this model may give a good description of nuclei that have a sizable number of both valence neutrons and valence protons, it has only a limited applicability to a near semiclosed shell nucleus like ^{144}Nd. The IBA should, however, still be applicable to the most collective states in ^{144}Nd, such as the ground state and the 2_1^+ state. Thus we have established a relationship between the CVM and IBA models. Their relationship can in turn be used to give a more simplified interpretation of the states calculated in the CVM, such as the assignment of a neutron-proton symmetry character.

It is important to recognize that, in the sense of boson symmetry, the present study opens up the possible extension of CVM itself. In the CVM, the quadrupole boson space is truncated at a certain boson number N (e.g., $N=3$ for the present calculation of ^{144}Nd), and the matrix elements between the quadrupole boson states are independent of N. These boson characteristics appear in the standard quadrupole models.[44] However, there is a simple way to introduce the N dependence in the matrix elements of each term in the Hamiltonian by keeping all $b^\dagger b$ terms unchanged and replacing additional $b^\dagger$ or b operators (where they appear) by $b^\dagger(N-\hat{N})^{1/2}$ or $(N-\hat{N})^{1/2}b$, respectively. Here $b^\dagger$ is the creation operator for the quadrupole boson and $\hat{N}=\sum_\mu b_\mu^\dagger b_\mu$ is the number operator. The ensuing model is characterized by the SU(6) symmetry, analogously to IBA, and is referred to as the truncated quadrupole phonon model (TQM).[45] If one keeps only the most important terms, TQM is equivalent to IBA-1,[26,38,46] i.e., by a simple unitary transformation it can be brought to the well-known form of IBA-1. In a similar way, by introducing the boson truncation factor $(N-\hat{N})^{1/2}$ in the Hamiltonian, the standard particle-vibration model is generalized to a form which is equivalent to the interacting boson fermion model (IBFA).[38] Analogously, the CVM can be generalized to a model having an IBA type of boson core and an IBFA s type of coupling between the boson core and each fermion of the cluster; hence, it is referred to as the CIBA (i.e., the cluster IBA). As pointed out earlier, the relation among these models is shown schematically in Fig. 5.

ACKNOWLEDGMENTS

This work was supported, in part, by the U.S. Department of Energy under Contract No. W-7405-Eng-48 and the U.S. Yugoslav Joint Fund for Scientific and Technological Cooperation, in cooperation with the U.S. National Science Foundation under Grant No. JFP-381/NSF. One of us (S.B.) would like to thank the Alexander von Humboldt Foundation for financial support.

*On leave of absence from the University of Zagreb.

[1]W. D. Hamilton, A. Irbäck, and J. P. Elliott, Phys. Rev. Lett. **53**, 2469 (1984).
[2]J. Dalmasso, H. Forrest, and G. Ardisson, Phys. Rev. C **32**, 1006 (1985).
[3]K. S. Krane, S. Raman, and F. K. McGowan, Phys. Rev. C **27**, 2863 (1983).
[4]M. K. Harder, W. D. Hamilton, G. Colvin, and A. R. H. Subber, in *Nuclear Structure, Reactions, and Symmetries*, edited by R. A. Meyer and V. Paar (World Scientific, Singapore, 1986), p. 676.
[5]D. M. Snelling, Ph.D. thesis, University of Sussex, 1983 (unpublished); D. M. Snelling and W. D. Hamilton, J. Phys. G **9**, 763 (1983).
[6]J. K. Tuli, Nucl. Data Sheets **56**, 607 (1989).
[7]T. J. Al-Janaby, J. D. Jafar, K. M. Mahmood, H. M. Youhana, A. M. Demidov, and L. I. Govor, Nucl. Phys. **A402**, 247 (1983).
[8]M. S. Pavikoff, G. Barci-Funcl, and G. Ardisson, Radiochem. Radioanal. Lett. **40**, 123 (1979).
[9]J. K. Tuli, Nucl. Data Sheets **27**, 97 (1979).
[10]*Tables of Isotopes*, 7th ed., edited by C. M. Lederer and V. S. Shirley (Wiley, New York, 1978).
[11]S. Raman, O. Shahl, D. A. McClure, and M. J. Kenny, Proceedings of the Conference on Neutron Capture, Gamma-Ray Spectroscopy, and Related Topics [Inst. Phys. Conf. Ser. **62**, 435 (1981)].
[12]R. Chapman, W. McLatchie, and J. E. Kitching, Nucl. Phys.

A186, 603 (1972).
[13]P. D. Bond, in *Nuclei of the Line of Stability,* edited by R. A. Meyer and D. S. Brenner (American Chemical Society, Washington, D.C., 1986), p. 335.
[14]J. P. Collins, C. T. Wunker, R. L. Place, and D. R. Ober, Bull. Am. Phys. Soc. **21**, 149 (1976).
[15]W. Behar, Z. W. Grabowski, and S. Raman, Nucl. Phys. **A219**, 516 (1974).
[16]J. B. Ball, R. L. Auble, J. Rapaport, and C. B. Fulmer, Phys. Lett. **30B**, 533 (1969).
[17]S. Raman, R. L. Auble, J. B. Ball, E. Newman, J. C. Wells, Jr., and J. Lin, Phys. Rev. C **14**, 1381 (1976).
[18]H. Wiegmann, G. Rohr, and M. Heske, Nucl. Phys. **A185**, 229 (1972).
[19]D. Rabenstein, Ya.Ya. Berzin, A. E. Kruminya, and P. T. Prokofe'v, Izv. Akad. Nauk SSSR, Ser. Fiz. **40**, 68 (1976).
[20]Ya.Ya. Berzin, M. R. Beitin, A. E. Kruminya, P. T. Prokofe'v, H. Rotter, H. Heiser, F. Stari, and V. Paar, Izv. Akad. Nauk SSSR **40**, 1193 (1976).
[21]D. Bohle, A. Richter, W. Steffen, A. E. L. Dieperink, N. Lo Iudice, F. Palombo, and O. Scholten, Phys. Rev. Lett. **137B**, 27 (1984).
[22]E. A. Henry, in *Nuclear Structure, Reactions, and Symmetries,* edited by R. A. Meyer and V. Paar (World Scientific, Singapore, 1986), p.616.
[23]R. A. Meyer, E. A. Henry, A. Aprahamian, L. G. Mann, S. Brant, V. Paar, and O. Scholten, Lawrence Livermore National Laboratory Report UCAR 10062/86, 1986, pp. 4–58.
[24]K. Heyde and J. P. Brussard, Nucl. Phys. **A104**, 81 (1967).
[25]G. Vanden Berghe, Z. Phys. A **272**, 245 (1975).
[26]A. Arima and F. Iachello, Ann. Phys. (N.Y.) **99**, 253 (1976).
[27]A. Arima and F. Iachello, in *Advances in Nuclear Physics,* edited by M. Baranger and E. Vogt (Plenum, New York, 1984), Vol. 13, p. 139.
[28]B. J. Raz, Phys. Rev. **114**, 1116 (1959).
[29]G. Alaga and G. Ialongo, Phys. Lett. **22**, 219 (1966).
[30]V. Paar, Nucl. Phys. **A221**, 29 (1973).
[31]O. Scholten, Ph.D. thesis, University of Groningen, 1980.
[32]V. Paar, in *Problems of Vibrational Nuclei,* edited by G. Alaga, V. Paar, and L. Šips (North-Holland, Amsterdam, 1975), p. 15.
[33]L. S. Kisslinger and R. A. Sorensen, Rev. Mod. Phys. **35**, 853 (1963).
[34]W. Booth, S. Wilson, and S. S. Ipson, Nucl. Phys. **A229**, 61 (1974).
[35]V. Paar, Z. Phys. A **271**, 11 (1974).
[36]G. Alaga, V. Lopac, and V. Paar, Phys. Lett. **43B**, 459 (1973).
[37]A. Bohr and B. Mottelson, *Nuclear Structure* (Benjamin, New York, 1972), Vol. II.
[38]V. Paar, S. Brant, L. F. Canto, G. Leander, and M. Vouk, Nucl. Phys. **A378**, 41 (1982).
[39]V. Paar, in *Heavy-ions, High-spin States and Nuclear Structure* (IAEA, Vienna, 1975), Vol. 2, p. 179.
[40]P. Van Isacker, K. Heyde, M. Waroquier, and G. Wenes, Nucl. Phys. **A380**, 383 (1982).
[41]O. Scholten, K. Heyde, P. Van Isacker, J. Jolie, J. Moreau, M. Waroquier, and J. Sau, Nucl. Phys. **A438**, 41 (1985).
[42]T. Otsuka, A. Arima, F. Iachello, and I. Talmi, Phys. Lett. **76B**, 139 (1979).
[43]F. Iachello, Phys. Rev. Lett. **53**, 1427 (1984).
[44]G. Gneuss and W. Greiner, Nucl. Phys. **A171**, 449 (1971).
[45]D. Janssen, R. V. Jolos, and F. Dönau, Nucl. Phys. **A224**, 93 (1974).
[46]A. Klein and M. Vallieres, Phys. Lett. **98B**, 459 (1973).